SLP Optimization-Based Voltage Profile Improvement in Unbalanced Distribution Networks

Mohammed Bamatraf
Department of Electrical Eng.
Istanbul Technical University
Turkey
matraf21@itu.edu.tr

Oğuzhan Ceylan
Dept.of Electrical and Electronics Engineering
Marmara University, Turkey
Oguzhan.ceylan@marmara.edu.tr

Ioana Pisica
Dept.of Electrical and Computer Eng
Brunel University, London, UK
Ioana.pisica@brunel.ac.uk

Aydoğan Özdemir
Department of Electrical Eng.
Istanbul Technical University,
Turkey
ozdemiraydo@itu.edu.tr

***Abstract*—Because of their advantages, active distribution networks implement renewable energy resources (RERs) such as photovoltaic units and wind turbines. However, there may be some drawbacks due to the intermittent nature of RERs, such as voltage fluctuations and increased system losses. This paper presents an optimization process that is solved by sequential linear programming to improve the voltage profile of the distribution network. The proposed optimization method is applied to a modified IEEE 34 Bus Test system. The method optimizes the voltage deviations by changing the taps of the voltage regulators and the reactive power injected by the inverters of the PV systems. The voltage profiles of the base case and optimal case are compared at different hours of the day with varying active and reactive loads and PV outputs. Simulation results done by MATLAB show that the proposed approach can provide a better voltage profile.**

Keywords— Renewable energy resources, photovoltaic Systems, active distribution networks.

I. INTRODUCTION

The use of renewable energy resources such as photovoltaic (PV) systems and wind turbines (WTs) is characterized by the irregular and intermittent nature of their output power. Inappropriate integration of these sources into distribution networks (DNs) often causes bus voltage limit violations, leading to higher system losses. Hence, control-related measures must be considered before integrating renewable energy resources into the distribution grid [1].

Switching-based devices like voltage regulators and capacitor banks have been utilized to regulate voltage profiles and reactive power flows in distribution networks for a long time. However, the increasing integration of RERs has made it challenging for traditional regulating devices to maintain the desired voltage profiles and power flows. Additionally, frequent switching actions significantly impact these devices' lifecycle and performance [2]. In this regard, inverter-interfaced DERs are the promising alternative to improve voltage profiles and ensure the stability of the DN by providing necessary voltage/VAR control, which would decrease the switching actions of the regulators and capacitor banks.

Control-related considerations play a crucial role in enhancing the efficiency of active distribution networks (ADNs) by implementing novel strategies to coordinate all DERs integrated into the network, leading to improved system operation [3]. The management and optimization process of ADNs involve solving optimal power flow equations that ensure minimal production costs for DG units while minimizing several other objective functions [4].

DN optimal power flow problems have been addressed using heuristic solution algorithms [5-7] and nonlinear programming methods [8-10]. Direct solutions to nonlinear programming problems have been achieved using gradient search and interior point methods. However, these methods require longer computation times than the time constraint for real-time controls [11]. Faster methods have been proposed by linearizing the optimization problem. However, this may cause oscillation around non-optimal points and fail to converge to the global optimal solution [12-14].

In [15], the author mentioned how SLP was used to solve OPF, which had many desirable characteristics such as reliability, speed, and good convergence with high-scale problems. SLP has also been used in [16] to coordinate switched capacitors and OLTC with droop control of smart inverter. This study presents another analytical approach that is supposed to be faster than heuristic methods and provide local optimal solutions. The proposed sequential linear programming (SLP) improves the voltage profiles in an unbalanced distribution network by controlling tap changers and reactive power flow from the smart inverter of multiple PV units at every time step. The effectiveness of the proposed method is demonstrated on the IEEE 34-bus unbalanced feeder.

Sections II and III of this paper will focus on formulating the optimization problem and the test system for the SLP method, respectively. Implementation of SLP optimization is introduced in Section IV: Section V shows simulation results, and Section VI concludes the paper.

II. PROBLEM FORMULATION

The details of the nonlinear constrained optimization problem formulation are introduced below.

A. Objective Function (OF)

The main objective of the study is to improve the voltage profiles of the distribution network (DN) by minimizing the deviations in voltage magnitudes from a flat value of 1 pu. Mathematically, this objective is formulated in (1):

$$OF = Norm\ [\mathbf{1} - \boldsymbol{V}] \tag{1}$$

where the vector $\boldsymbol{V} = [\boldsymbol{V_1}, \boldsymbol{V_2}, \ldots, \boldsymbol{V_n}]^{\mathrm{T}}$ represents the voltage magnitudes of feeder busses for all three phases, and $\mathbf{1}$ denotes a vector of the same dimension whose all entries are 1. It is important to note that n is 165 for the IEEE-34 node feeder, which includes all three phases for original and additional nodes. More is explained further in Sec II. The Norm in the equation refers to the Euclidean norm of a vector.

B. Equality Constraints (EC)

The equality constraints are the unbalanced power flows, solved by the iterative forward-backward sweep method (FBSM) [17]. Equation (2) shows the relation-ship between the constraints and the control variables:

$$\boldsymbol{V} = PowerFlow\ [\boldsymbol{X}] \tag{2}$$

2023 International Conference on Smart Energy Systems and Technologies (SEST) | 979-8-3503-9790-1/23/$31.00 ©2023 IEEE | DOI: 10.1109/SEST57387.2023.10257319

X here denotes the control variable vector, which consists of the reactive power output of the smart inverters and the positions of the tap transformers. Let us consider a section of a radial feeder shown in Fig. 1 to explain the forward-backward iterative method. The nodes are enumerated from 1 (starting point) to n (endpoint).

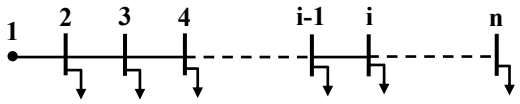

Fig. 1. One phase of a radial feeder.

For the known branch impedances and loads, the FBSM starts by assigning an initial voltage value to the end node-n and uses Kirchoff's current law to calculate the current at node-n, as expressed in (3).

$$\dot{I}_n = \frac{\dot{V}_n}{\dot{Z}_n} \tag{3}$$

where $\dot{V}, \dot{I}$ *and* $\dot{Z}$ represent the bus voltage, branch current, and branch impedance phasors. The i and (i-1) in Fig.1 refer to the successive busses along the same phase. The previous node's voltage is then calculated by Kirchoff's voltage law as expressed in (4). Eq. (5) refers to the line current equation used while moving backward.

$$\dot{V}_{n-1} = \dot{V}_n + \dot{Z}_{n-1,n} * \dot{I}_{n-1,n} \tag{4}$$

$$\dot{I}_{n,n-1} = \dot{I}_n + \dot{I}_{n+1,n} \tag{5}$$

This process is repeated for all the nodes up to the starting node-1. Check the stopping criteria in (6). The iteration stops if the condition is satisfied. Otherwise, it continues with the forward direction by calculating the node voltages after assigning the first node the reference value and then using (4) to calculate $\dot{V}_2$ and using the line current found earlier in the backward process.

$$|\dot{V}_{1calc} - \dot{V}_{1ref}| \leq \epsilon \tag{6}$$

Note that during this process $\dot{V}_{n-1}$ is known and $\dot{V}_n$ is the unknown in (4) and $\dot{I}_{n,n-1}$ is known and $\dot{I}_{n+1,n}$ is unknown in (5). This forward process continues until reaching node n and then again moving backward using the same first steps until reaching node 1. and checking if the criteria in (6) are satisfied.

C. Inequality Constraints (IC)

The inequality constraints are based on the permissible limits of the bus voltage magnitudes. It is assumed that the line flows are not critical in a distribution feeder. The magnitudes of the feeder bus voltages are desired to remain within the range of 0.95 to 1.05 pu. A viable approach to formulate the inequality constraint involves verifying whether the voltage magnitude of each node violates the acceptable limits. The formulation represented in (7):

$$G_i^j(V_i) = \begin{Bmatrix} 0.95 - V_i & if & V_i < 0.95 \\ 0 & if & 0.95 \leq V_i \leq 1.05 \\ V_i - 1.05 & & V_i > 1.05 \end{Bmatrix} \tag{7}$$

In (7), the subscripts i and j refer to the per-phase voltage enumeration and simulation time, respectively. A suitable expression for the inequality constraint is expressed as follows:

$$\mathrm{G}^j(\mathbf{V}) = \sum_{i=1}^{n} G_i^j(V_i) \tag{8}$$

Therefore, the final formulation of the constrained optimization problem is presented as follows:

$$\begin{matrix} Minimize & OF = \mathrm{Norm}\,[\mathbf{I} - \mathbf{V}] \\ & \boldsymbol{V} = PowerFlow\,[\boldsymbol{X}] \\ Subject\ to & \mathrm{G}^j(\mathbf{V}) \leq 0 \end{matrix} \tag{9}$$

D. Control Variables (CV)

Two control variables are optimized to obtain the best voltage profiles during the optimization process.

1) Reactive power support from PV units (inverter)

PV systems are typically equipped with smart inverters that facilitate a bidirectional reactive power flow in addition to DC to AC conversion. The control parameters of an inverter is a vector with three values, one for each phase, as shown in (10). It should be noted that the inverter can provide reactive power support from the PV system only when active power generation is available. Here, we assume that the inverter can support reactive power when its active power generation is greater than 5% of the rated value.

$$Q = [Q_a\ Q_b\ Q_c]^T = [X_1\ X_2\ X_3]^T \tag{10}$$

In this study, phase reactive powers (Q_a , Q_b, and Q_c) are limited to a range of -120 kVAr to 120 kVAr, or -90 kVAr to 90 kVAr, depending on the rating of the PV unit. Note that the reactive power consumption or injection is limited by the power balance equation shown in (11), which varies depending on the PV panels' active power generation during the day. It is also constrained by a minimum power factor of 0.95. The following section provides more details about the constraints on the reactive power.

$$Q = \sqrt{S^2 - P^2} \tag{11}$$

2) Tap positions of the voltage regulators

There are two regulating transformers (tap changers) between the nodes 814-850 and 832-854 in the feeder. Those tap positions values are included in the optimization problem as three-valued control vectors. It is important to note that the values in the vector will only be integers since the tap positions are fixed and each position can only change the corresponding voltage by a specific ratio of 0.0625 pu.

$$T_1 = [X_4\ X_5\ X_6]^T\ T_2 = [X_7\ X_8\ X_9]^T \tag{12}$$

III. Test System

A. IEEE 34 Node Test Feeder

The IEEE 34-Bus Test System is an unbalanced radial system that is commonly used for distributed generation studies [18]. The single-line diagram of the modified test system, including the locations of the tap positions and the PV units, is shown in Fig. 2.

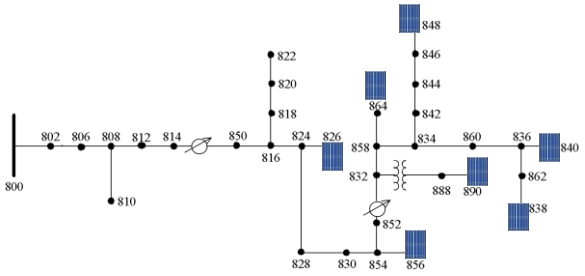

Fig. 2. IEEE-34 node test feeder and locations of PV units.

B. High PV penetration

Seven PVs are integrated into the DN. The size of the PV unit at node 890 was chosen to be 120 kW since this node shows the lowest voltage level. The size of the other six units were selected to be 90 kW. The allocation criteria for these units are based on the voltage level at the nodes. Since the right-hand side nodes are far from the supply point, they need reactive power support to compensate for their voltage drops. However, because of high PV penetration, there is a risk of overvoltages, especially during high irradiation time. On the other hand, it is much more efficient if the PV units are distributed among the nodes rather than concentrated at one node or a few nodes with a large amount of PV injection [19].

C. Load profile

The system includes 99 prospective load buses (3*33), with the first grid connection point is assumed to be load-free. However, there are some distributed loads along the lines. So, the midpoint is considered a new dummy bus that carries half the load, and the other half is added to the next bus. The resulting total number of busses is 55 per phase. Table 1 illustrates the nodes comprising the loads.

TABLE I. DISTRIBUTION SYSTEM SPOT LOADS.

Node #	Active Power (kW)			Reactive Power (kVAr)		
	a	b	c	a	b	c
830	10	10	25	5	5	10
890	150	150	150	75	75	75
844	135	135	135	105	105	105
860	20	20	20	16	16	16
848	20	20	20	16	16	16
840	9	9	9	7	7	7

During the initial phase of this study, all nodes are assumed to follow an identical load pattern depicted in Fig. 3 [20]. However, to account for the unpredictable nature of the load, a 5% random deviation from the rated data is factored into each simulation. In this regard, random coefficients within the ±5%range of the limits are used.

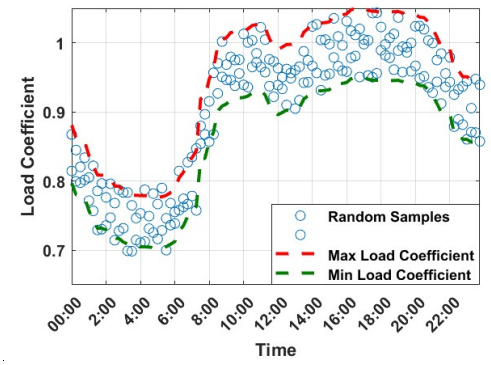

Fig. 3. Scaled load pattern for the distribution system.

D. Photovoltaic Units

The PV units installed in the test system have two different ratings: 120 kW at node 890 and 90 kW at other busses. The daily active power generation data for the 120 kW PV unit with a 15-minute time resolution is illustrated in Fig. 4. Additionally, the reactive power calculated using (11) has been adjusted to comply with a minimum power factor of 0.95. This modification is mathematically expressed in (13). Fig. 4 shows the active power generation throughout the day and the maximum amount of reactive power that can be injected or consumed at every step [21].

$$Q = Min\{\sqrt{S^2 - P^2}, P * \tan(\emptyset)\} \quad \emptyset = cos^{-1}0.95 \quad (13)$$

Note that Fig. 4 shows the characteristics of only the 120 kW PV unit at node 890. The characteristics of the active power and reactive power for the six PVs at other nodes follow the same behavior.

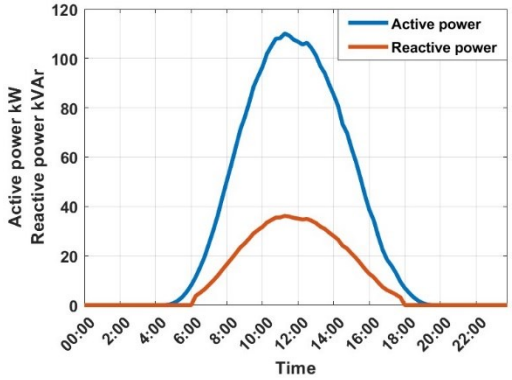

Fig. 4. PV output power for a constant power factor.

IV. Implementation of SLP Optimization

SLP is a very efficient method for solving constrained nonlinear optimization problems. At first, the objective function and constraints are linearized around an operation point. Then, a basic linear programming method is used to obtain the optimal solution to the linearized problem. Equation (9) gives the formulation of the optimization problem to be solved using SLP. The control vector comprises the reactive power outputs of PV units and tap positions of the regulating transformer:

$$X = [Q_{120}^T\ T_1^T\ T_2^T\ Q_{90}^T] \quad (14)$$

$$Q_{120}^T = [X_1\ X_2\ X_3]^T \quad (15)$$

$$T_1 = [X_4\ X_5\ X_6]^T\ T_2 = [X_7\ X_8\ X_9]^T \quad (16)$$

$$Q_{90}^T = [X_{10}\ X_{11} \dots X_{27}]^T \quad (17)$$

Bus voltages of the phases are the state variables that are expected to be within the specified limits.

$$V_{min} \le V = [V_1\ V_2 \dots V_{165}]^T \le V_{max} \quad (18)$$

The steps to solve the above optimization problem using SLP are as follows [22].

Step-1 A feasible initial control vector x_0 is assigned; the objective function and the constraints are linearized around that point. The linearized version of the objective function $F(x)$can be expressed as follows;

$$\tilde{F}(x) = F(x_0) + \nabla F(x_0)^T * x \quad (19)$$

where ∇ is the gradient operator.

Step-2 The inequality constraint function $G(x)$ is linearized around the control vector.

$$\tilde{G}(x) = G(x_0) + \nabla G(x_0)^T * x \quad (20)$$

Step-3 A basic linear programming method like simplex is used to solve the following optimization problem.

$$Minimize\ \tilde{F}(x)\ Subject\ to\ \tilde{G}(x) \le 0 \quad (21)$$

Step-4 This step updates the operating control vector by adding the solution of Eq. (21)

$$x_{new} = x_0 + x_{sol} \quad (22)$$

Step-5 Repeat the steps from 2 until one of the following criteria is satisfied.

$$|x_{new} - x_{old}| \leq \in \; or \; |F(x_{new}) - F(x_0)| \leq \in \quad (23)$$

where $\in$ is a tolerance value such as 0.0001.

V. Simulation Results

MATLAB was used to show the results illustrated in Figs. 7-11 by plotting the voltage profiles of the nodes for the base and optimal operation cases on the same figure. Note that all bus voltages for all phases are plotted (165) bus values, but only few names are lebeld in the x axes for visual clarity. The values of the control variables are also illustrated in Figs. 12-14.

Fig. 5 shows the voltage profiles without any PV and tap actions (base case). That is, all voltage regulator taps are set to position 0, and reactive power flow injection/absorption to/from the inverter is 0. Note that there are many undervoltage violations for this operating case.

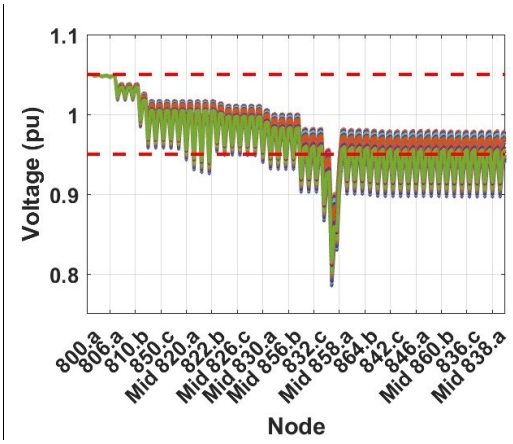

Fig. 5. Base case voltage profiles for 24 hours

Fig. 6 shows the effect of high PV generation on the voltage profiles, while the tap positions are still 0 and the PV units have no reactive power support. There are some overvoltages at some hours because of high PV injections, while still some undervoltages at some hours because of insufficient reactive power supply and regulator support.

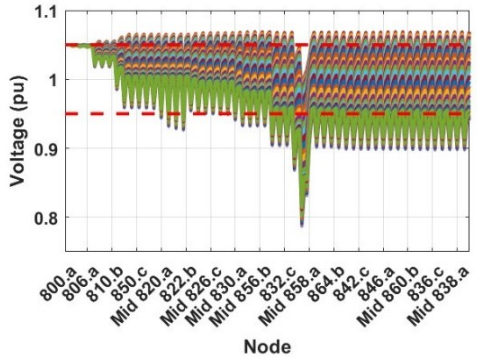

Fig. 6. Voltage profiles for 24 hours with high PV penetration.

The optimization problem formulated by (9) is solved using the SLP to minimize the number of undervoltage problems and their severity that appear early in the morning and late in the day. Moreover, SLP is also supposed to minimize the overvoltage problems occurring during noon due to the high solar radiation (active power generation). The results are illustrated for some representative hours.

A. Simulation results at 12 a.m.

Simulation results for 12 a.m. are illustrated in Fig. 7. The PVs are not active at this hour. Voltage profiles are controlled by only optimizing the voltage regulator taps. A comparison of base and optimal case results shows that the voltage regulators can eliminate all the undervoltage problems. In contrast, some node voltages approach their upper limits. The same behavior is valid up to 6 a.m.

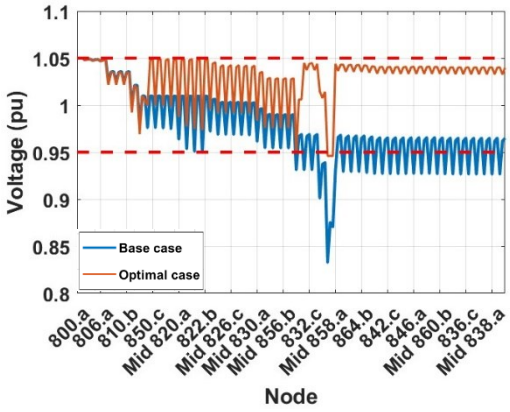

Fig. 7. Base case and optimal voltage profiles at 12 a.m.

B. Simulation results at 7 a.m.

PV units can provide a limited amount of reactive power support at 7 a.m. SLP optimizes the regulator taps and reactive power support from the inverter to solve the undervoltage problems.

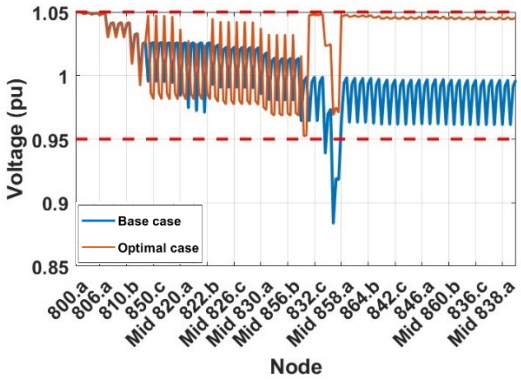

Fig. 8. Base case and optimal voltage profiles at 7 a.m.

C. Simulation results at 9 a.m.

PV units have enough reactive power capacity to solve the undervoltage problems. The SLP method optimizes only the reactive power injected from the inverter without any tap control actions. Fig. 9 show that all the undervoltage problems are eliminated while preventing abnormal increases in other buses. Note that the reactive power capacity of PV units is always sufficient for the mentioned voltage control for the period between 9 a.m. to 3 p.m.

D. Simulation results at 12 p.m.

At this time, the power generation form the PVs is at its maximum. Almost all the busses experience overvoltage

problems. SLP uses only inverter reactive power to solve overvoltages and undervoltage at 890 as shown in Fig. 10.

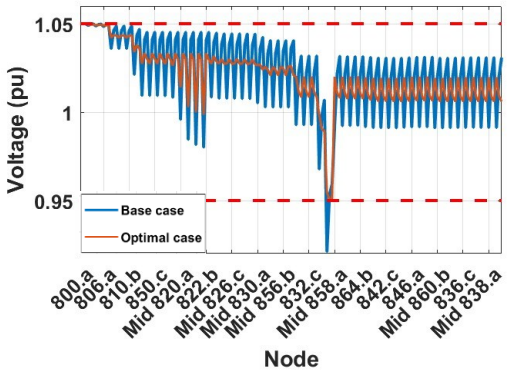

Fig. 9. Base case and optimal voltage profiles at 9 a.m.

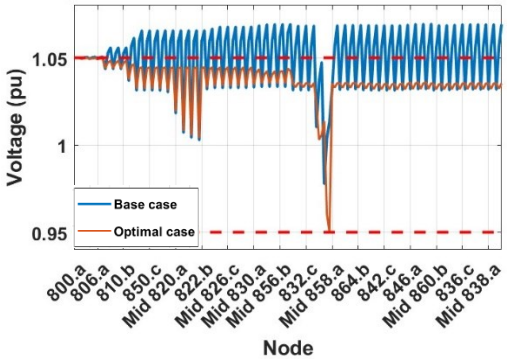

Fig. 10. Base case and optimal voltage profiles at 12 p.m.

E. Simulation results at 5:30 p.m.

At 5:30 p.m. and later, the SLP method cannot eliminate all the undervoltage problems as there is not enough PV reactive power support, and the regulators are insufficient because the load is at its highest value. A reactive power source, a shunt capacitor, at node 890 can alleviate the problem. The results are illustrated in Fig. 11.

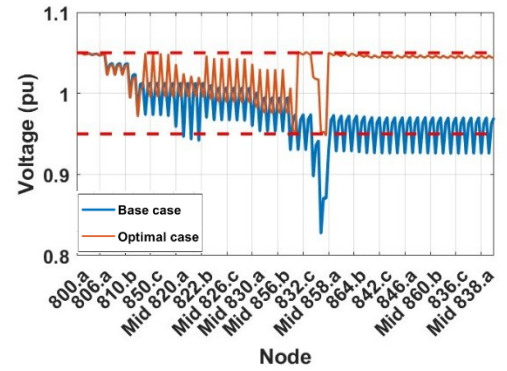

Fig. 11. Base case and optimal voltage profiles at 5:30 p.m.

F. Reactive power output from inverter at node 890

Fig. 12 shows the reactive power output of the PV unit installed at node 890. It is observed that in the morning, the inverter injects reactive Power to solve the undervoltage at node 890. During the high solar irradiation period, noon time, there are overvoltage violations almost at all the nodes. Therefore, PV at 890 consumes reactive power to bring the voltage down to the allowable limit. In the afternoon, as the sun goes down, there is no more overvoltage problem, the bus voltages decrease, and the undervoltage problem starts at node 890. That is why the reactive power is now injected to bring the voltage up. Note that other reactive power outputs for 90 kW inverter have the same behavior as the 120 kW. However, they were not plotted as they would increase the number of figures in the paper.

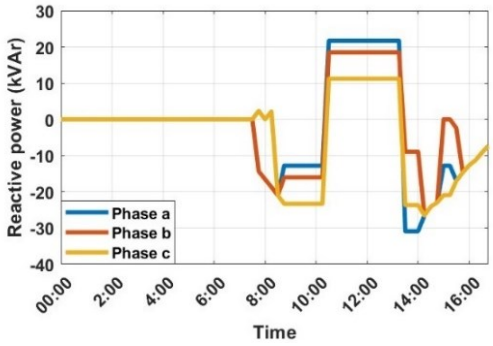

Fig. 11. Reactive power flow from the inverter at 890.

G. Reactive Power from inverters of other nodes.

Fig. 13 shows the set of reactive power output of the PV units installed at other nodes. Those are 6 PV units with 90 kVAr power rating which make 18 overall plots in the figure. Some follow the same behavior as that of 120 kVAr for the same reasons. However, since the voltage deviation at other nodes is not as high as that at 890, some inverters consume 0 reactive power as shown in Fig. 13 between 9-3 p.m. because otherwise, it would result in reducing too much voltage level for those nodes.

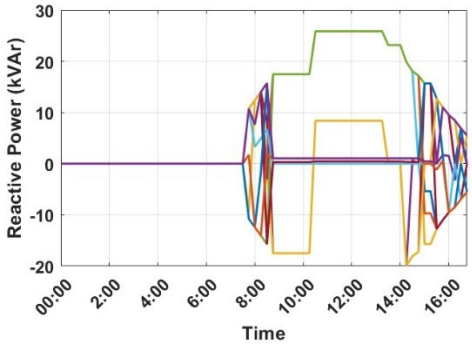

Fig. 12. Reactive power flow from the inverter other nodes.

H. Voltage Regulators

Fig. 14 and Fig. 15 show how the tap positions of regulating transformers change during the day. Note that since the reactive power from the PV units is sufficient for the voltage control between 9:00 a.m. -3:00 p.m. voltage regulators are kept at zero positions to extend their lifecycle.

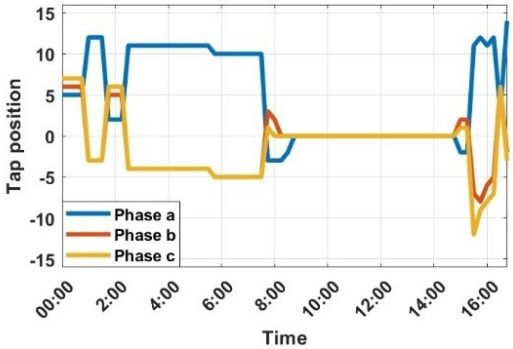

Fig. 13. Optimal positions of Regulator-1 along the day

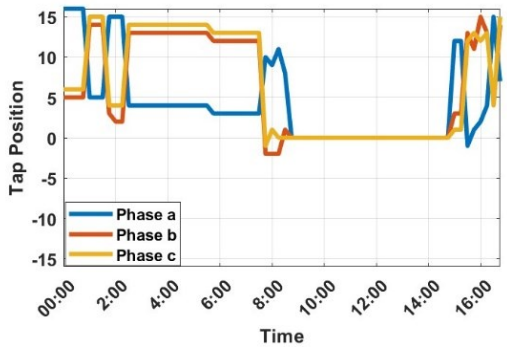

Fig. 14. Optimal positions of Regulator-2 along the day

VI. Conclusions

This study has presented an approach to improve voltage profiles in an unbalanced distribution network by controlling tap changers and reactive power flow from the smart inverter of multiple PV units. The SLP method was used to solve the optimization equations at each time step. The effectiveness of the proposed approach was demonstrated on the IEEE 34-bus unbalanced feeder. The results show that the proposed formulation and SLP implementation has successfully maintained the voltage profile within the allowable limits from 12 a.m. to 5:30 p.m. Tap positions of the regulating transformers were sufficient to succeed in the intended tasks without any PV reactive power support from midnight up to early morning since the load level was not high. The integration of multiple PV units contributed to solving the overvoltage problems and maintaining the voltage profile within the required limits without voltage regulator support from 9:00 a.m. to 3:00 p.m. However, regulating transformers failed to solve the undervoltage problems after 5 p.m. because of insufficient reactive power support from PV units and high load levels. At this point, shunt capacitor banks installation seemed to be an alternative, at least to alleviate the problem.

The study also showed that the proposed control actions ensure more reliable system operating conditions. Moreover, the tap regulation is not needed for a specific time of the day when the reactive power support is enough to obtain an optimal voltage profile. The simulation time ranges between 5-16 seconds, which makes it a good choice for online strategies in active distribution networks.

Acknowledgment

This research is funded as a part of "120N996 Implementing digitalization to improve energy efficiency and renewable energy deployment in Turkish distribution networks" project under the framework of 2551 Project organized by TUBITAK and the British Council.

References

[1] J. A. P. Lopes, N. Hatziargyriou, J. Mutale, P. Djapic, and N. Jenkins, "Integrating distributed generation into electric power systems: A review of drivers, challenges and opportunities," Elect. Power Syst. Res., vol. 77, no. 9, pp. 1189–1203, 2007.

[2] Y. P. Agalgaonkar, B.C. Pal and R.A. Jabr, "Distribution Voltage Control Considering the Impact of PV Generation on Tap Changers and Autonomous Regulators," IEEE Trans. Power Syst., vol. 29, no. 1, pp. 182-192, Jan. 2014.

[3] Y. Zhu and K. Tomsovic, "Optimal Distribution Power Flow for Systems with Distributed Energy Resources," Int. J. Elect. Power Energy Syst., vol. 29, no. 3, pp. 260-267, Mar. 2007.

[4] Ahmadi, B., Ceylan, O., Ozdemir, A., "Grey wolf optimizer for allocation and sizing of distributed renewable generation", 54rd International Universities Power Engineering Conference, September 3-6 2019, Bucharest, Romania.

[5] Ahmadi, B., Ceylan, O., Ozdemir, A., "Distributed energy resource allocation using multi-objective grasshopper optimization algorithm," Electric Power Systems Research, Volume 201, Article Number107564.

[6] Ahmadi, B., Ceylan, O., Ozdemir, A., Fotuhi-Firuzabad, M., "A multi-objective framework for distributed energy resources planning and storage management," Applied Energy, 314(1):118887, May 2022.

[7] Ahmadi B, Ceylan O, Ozdemir A. A multi-objective optimization evaluation framework for integration of distributed energy resources. J Energy Storage 2021; 41:103005.

[8] S. Gill, I. Kockar and G.W. Ault, "Dynamic Optimal Power Flow for Active Distribution Networks," IEEE Trans. Power Syst., vol. 29, no. 1, pp. 121-131, Jan. 2014.

[9] Y. Zhu and K. Tomsovic, "Optimal Distribution Power Flow for Systems with Distributed Energy Resources," Int. J. Elect. Power Energy Syst., vol. 29, no. 3, pp. 260-267, Mar. 2007.

[10] N. Daratha, B. Das and J. Sharma, "Coordination Between OLTC and SVC for Voltage Regulation in Unbalanced Distribution System Distributed Generation," IEEE Trans. Power Syst., vol. 29, no. 1, pp. 289-299, Jan. 2014.

[11] G. Liu, O. Ceylan, Y. Xu and K. Tomsovic, "Optimal voltage regulation for unbalanced distribution networks considering distributed energy resources," 2015 IEEE Power & Energy Society General Meeting, Denver, CO, USA, 2015, pp. 1-5, doi: 10.1109/PESGM.2015.7286473.

[12] A. Borghetti, M. Bosetti, S. Grillo, S.Massucco, C. Nucci,M. Paolone,and F. Silvestro, "Short-term scheduling and control of active distribution systems with high penetration of renewable resources," IEEE Syst. J., vol. 4, no. 3, pp. 313–322, Sep. 2010.

[13] Q. Zhou and J.Bialek, "Generation curtailment to manage voltage constraints in distribution networks," IET Gener., Transm., Distrib., vol. 1, no. 3, pp. 492–498, May 2007.

[14] V. Calderaro, G. Conio, V. Galdi, G. Massa and A. Piccolo, "Optimal Decentralized Voltage Control for Distribution Systems with Inverter- Based Distributed Generators," IEEE Trans. Power Syst., vol. 29, no. 1, pp. 230-241, Jan. 2014.

[15] Q. Long, J. Wang, D. Lubkeman, N. Lu and P. Chen, "Volt-Var Optimization of Distribution Systems for Coordinating Utility Voltage Control with Smart Inverters," 2019 IEEE Power & Energy Society Innovative Smart Grid Technologies Conference (ISGT), Washington, DC, USA, 2019, pp. 1-5, doi: 10.1109/ISGT.2019.8791600.

[16] H. Mataifa, S. Krishnamurthy and C. Kriger, "Volt/VAR Optimization: A Survey of Classical and Heuristic Optimization Methods," in IEEE Access, vol. 10, pp. 13379-13399, 2022, doi: 10.1109/ACCESS.2022.3146366.

[17] W. H. Kersting and D. L. Mendive, "An application of ladder network theory to the solution of three phase radial load flow problems", IEEE PES Winter Meeting, 1976.

[18] IEEE 34 Node TestFeeder. "Distribution System Analysis Subcommittee Report." IEEE Transactions, 2003.

[19] O. Ceylan, S. Paudyal, B. Bhattarai and K. Myers, "Photovoltaic Hosting Capacity of Feeders with Reactive Power Control and Tap Changers", 2017 IEEE PES Innovative Smart Grid Technologies Conference Europe (ISGT-Europe), 2017.

[20] https://seffaflik.epias.com.tr/transparency/

[21] https://ideas.repec.org/a/eee/energy/v114y2016icp1251-1265.html.

[22] Venkataraman, P., 2009. Applied Optimization with MATLAB Programming, second ed. John Wiley and Sons, Hoboke